Inorg. Chem. **2004**, *43*, 739–746

Hyperfine Splittings in Spin-Frustrated Trinuclear Cu_3 Clusters

Moisey I. Belinsky*

School of Chemistry, Sackler Faculty of Exact Sciences, Tel-Aviv University, Tel Aviv, Ramat Aviv 69978, Israel

Received October 1, 2003

The hyperfine structures of the EPR spectra of the spin-frustrated and distorted Cu(II) trimers were calculated in the spin-coupling model. The correlations between the hyperfine structures of the EPR spectra and geometry of the Cu_3 clusters (equilateral, isosceles, and scalene triangles) were found. For the EPR spectrum of the spin-frustrated ground state $2(S = 1/2)$ of an equilateral triangle Cu_3 cluster ($J_{12} = J_{13} = J_{23} = J$), the calculated hyperfine structure represents the complicated spectrum of the 24 hyperfine lines, of total length 5*a*, where *a* is the hyperfine constant of the mononuclear Cu center. For an isosceles Cu_3 cluster ($J_{12} \neq J_{13} = J_{23}$), the hyperfine splittings of the EPR spectra of the two split $S = 1/2$ levels with intermediate spins $S_{12} = 0$ and $S_{12} = 1$ are essentially different. The EPR signal of the $|(S_{12} = 0)S = 1/2\rangle$ level is characterized by the four equally spaced hyperfine lines (interval $A = a$) with the same relative spectral amplitudes 16:16:16:16 and total length 3*a*. For the $|(S_{12} = 1)S = 1/2\rangle$ level, the calculated hyperfine structure represents the spectrum of the 16 hyperfine lines with equal spacing (interval $A' = a/3$), the spectral intensity distribution 1:1:3:3:5:5:7:7:7:7:5:5:3:3:1:1 and total length 5*a*. These hyperfine spectra differ from the hyperfine structure (10 lines with interval *a*/3) of the EPR signals of the excited $S = 3/2$ level of the Cu_3 cluster. The quartet hyperfine structure, characteristic of a single Cu^{2+} nucleus, which was observed experimentally for the doublet ground state of the spin-frustrated Cu_3(II) clusters, corresponds to the hyperfine structure of the EPR signal of the $|(S_{12} = 0)S = 1/2\rangle$ level. This hyperfine structure is evidence of the lowering of the Cu_3 cluster symmetry from trigonal to orthorhombic and the small splitting of the spin-frustrated $2(S = 1/2)$ ground state.

Introduction

Polynuclear clusters of paramagnetic ions attract great attention as active centers in biological systems and their synthetic analogues,[1] single molecular magnets,[2] and models for molecular magnetism.[3] Many trimeric, tetrameric, and more complicated clusters and rings of different transition metal ions M (M = Cu, Fe, Mn, Cr, Ni) demonstrate highly symmetric geometry. For example, many trimeric Cu_3(II) clusters,[4−19] Fe_3 and Cr_3 clusters of basic carboxilates,[9,20]

* E-mail: belinski@post.tau.ac.il. Phone: 972-3-640-79-42. Fax: 972-3-640-92-93.

(1) (a) Holm, R. H.; Kennepohl, P.; Solomon, E. I. *Chem. Rev.* **1996**, *96*, 2239. (b) Beinert, H.; Holm, R. H.; Münck, E. *Science* **1997**, *277*, 653. (c) Solomon, E. I.; Sandaram, U. H.; Machonkin, T. E. *Chem. Rev.* **1996**, *96*, 2563.

(2) (a) Thomas, L.; Lionti, F.; Ballou, R.; Gatteschi, D.; Sessoli, R.; Barbara, B. *Nature* **1996**, *383*, 145. (b) Friedman, J. R.; Sarachik, M. P.; Tejada, J.; Ziolo, R. *Phys. Rev. Lett.* **1996**, *76*, 3830. (c) Aubin, S. M. J.; Sun, Z.; Eppley, H. J.; Rumberger, E. M.; Guzei, E. A.; Folting, K.; Gantzel, P. K.; Rheingold, A. L.; Christou, G.; Hendrickson, D. N. *Inorg. Chem.* **2001**, *40*, 2127.

(3) (a) Kahn, O. *Molecular Magnetism*; VCH: New York, 1993. (b) *Molecular Magnetism: from Molecular Assemblies to the Devices*; Coronado, E., Delhaes, P., Gatteschi, D., Miller, J. S., Eds.; NATO ASI Series 321; Kluwer: Dordrecht, 1996.

(4) Beckett, R.; Colton, R.; Hoskins, B. F.; Martin, R. L.; Vince, D. G. *Aust. J. Chem.* **1969**, *22*, 2527.

(5) Sinn, E. *Coord. Chem. Rev.* **1970**, *5*, 313.

(6) Griffith, J. S. *Struct. Bonding (Berlin)* **1972**, *10*, 87.

(7) (a) Tsukerblat, B. S.; Novotortsev, V. M.; Kuyavskaya, B. Ya.; Belinsky, M. I.; Ablov, A. V.; Bazhan, A. N.; Kalinnikov, V. T. *Sov. Phys. JETP Lett.* **1974**, *19*, 277. (b) Tsukerblat, B. S.; Kuyavskaya, B. Ya.; Belinsky, M. I.; Ablov, A. V.; Novotortsev, V. M.; Kalinnikov, V. T. *Theor. Chim. Acta* **1975**, *38*, 131. (c) Belinsky, M. I.; Tsukerblat, B. S.; Ablov, A. V. *Dokl. Phys. Chem.* **1972**, *207*, 911.

(8) Butcher, R. J.; O'Connor, C. J.: Sinn, E. *Inorg. Chem.* **1981**, *20*, 537.

(9) (a) Tsukerblat, B. S.; Belinsky, M. I. *Magnetochemistry and Radiospectroscopy of Exchange Clusters*; Shtiintsa: Kishinev, USSR, 1983. (b) Tsukerblat, B. S.; Belinsky, M. I.; Fainzilberg, V. E. *Sov. Sci. Rev., Sect. B* **1987**, *9*, 337.

(10) (a) Banci, L.; Bencini, A.; Gatteschi, D. *Inorg. Chem.* **1983**, *22*, 2681. (b) Banci, L.; Bencini, A.; Dei, A. Gatteschi, D. *Inorg. Chem.* **1983**, *22*, 4018.

(11) (a) Chandhuri, P.; Karpenshtein, I.; Winter, M.; Bultzlaff, G.; Bill, E.; Trautwein, A. X.; Flörke, U.; Haupt, H.-J. *J. Chem. Soc., Chem. Commun*. **1992**, 321. (b) Colacio, E.; Dominguezz-Vera, J. M.; Escuer, A.; Klinga, M.; Kiverkaes, R.; Romerosa, A. *J. Chem. Soc., Dalton Trans.* **1995**, 343. (c) Hulsbergen, F. B.; Hoedt, R. W. H.; Verschooz, G. C.; Reedijk, J.; Spek, L. A. *J. Chem. Soc., Dalton Trans.* **1983**, 539.

10.1021/ic035141r CCC: $27.50
Published on Web 12/17/2003

possess trigonal symmetry. In the case of high symmetry of the cluster, the temperature dependence of magnetic susceptibility $\chi(T)$ ($\mu_{eff}(T)$) is described by the Heisenberg exchange interaction $H_0 = -2J\sum_{i,j} \hat{\mathbf{s}}_i\hat{\mathbf{s}}_j$ with equal exchange parameters $J_{ij} = J$. The exchange levels ($E(S) = -JS(S + 1)$) of symmetrical polynuclear clusters are highly degenerate: the total spin $S < S_{max}$ corresponds to two or more different intermediate spins S_{ij}[6,7,9] (the spin-frustration effect[3a,11a,13,20−23]). In the trinuclear clusters with the geometry of an equilateral triangle, the highly degenerate nS levels correspond to single $^{2S+1}$E or several $^{2S+1}$E, $^{2S+1}$A$_1$, and $^{2S+1}$A$_2$ trigonal multiplets.[6,7c,9] The high degeneracy or spin-frustration of the spin nS levels of the symmetrical pure Heisenberg model is very sensitive to the interplay between the exchange parameters, local anisotropy, and symmetry lowering. The non-Heisenberg exchange interactions, such as the Dzialoshinsky−Moriya antisymmetric exchange $H_{DM} = \sum\vec{\mathbf{D}}_{ij}[\vec{\mathbf{s}}_i \times \vec{\mathbf{s}}_j]$ and biquadratic exchange $H_{BE} = \sum j_{ij}(\vec{\mathbf{s}}_i\vec{\mathbf{s}}_j)^2$,[9] the "magnetic Jahn−Teller effect",[24,20a] split the spin-frustrated nS levels.

Exchange-coupled Cu_3(II) clusters in synthetic and native systems have been the subject of experimental and theoretical investigations.[1c,4−19,25−29] Cu_3(II) clusters with the geometry of an equilateral triangle and equal antiferromagnetic Heisenberg exchange parameters $J_{12} = J_{13} = J_{23} = J$, which results in the degenerate ground state $nS = 2(S = 1/2)$, represent the simplest case of the spin-frustrated clusters. Recently, the hyperfine structure of the EPR spectra of the spin-frustrated ground state with $S = 1/2$ of the trigonal Cu_3 clusters was observed.[16,19] The EPR spectra of the spin-frustrated ground state with $S = 1/2$ possess a quartet hyperfine structure,[19] characteristic of a single Cu^{2+} site, that was explained[19] by lowering the symmetry and localization of the repaired electron orbital on only one of the three nuclei of the Cu_3 trimer. It was supposed[19] that the hyperfine spectrum of the EPR signal of the ground spin-frustrated state $S_{total} = 1/2$ of an equilateral Cu_3 triangle consists of 10 hyperfine peaks. The complicated hyperfine multiplet, which was observed in EPR spectra of the $2(S = 1/2)$ ground state of the spin-frustrated Cu_3 cluster,[16] was not explained. The authors[16] suggested that this hyperfine structure may be formed by a spin delocalization between the three Cu atoms. The fine structure of the EPR spectra of the spin-frustrated Cu_3 cluster,[15] which was described by the mononuclear Cu hyperfine constant $A_{||}$, was not explained. For the distorted Cu_3 cluster,[29] the authors[29] suggested that the observed six hyperfine lines multiplet may be due to the superposition of $S = 1/2$ signals from two $S = 1/2$ levels with different intermediate spins of the isosceles Cu_3 trimer. For the trigonal and distorted Cu_3 clusters, the knowledge of the hyperfine structures, which correspond to the spin-frustrated $2(S = 1/2)$ state and separated two $S = 1/2$ levels, is required.

The model of the hyperfine splittings of the EPR signals for spin-frustrated trigonal and distorted Cu_3 clusters was not developed, which creates difficulties in an explanation of the observed hyperfine structures of the Cu trimers. The aim of this paper is the calculation of the hyperfine splittings of the EPR spectra of spin-frustrated Cu_3 clusters with the geometry of an equilateral triangle, comparison with the hyperfine splittings for the distorted (isosceles and scalene) Cu_3 clusters and experimentally observed hyperfine structures.

Spin-Coupling Model

The spin Hamiltonian of the Cu_3(II) trimer in the spin-coupling model[6] has the form

$$H = -2\sum_{i,j} J_{ij}\hat{\mathbf{s}}_i\hat{\mathbf{s}}_j + \sum_{i=1-3}(\beta\hat{\mathbf{s}}_i\tilde{\mathbf{g}}_i\mathbf{H} + \hat{\mathbf{s}}_i\tilde{\alpha}_i\hat{\mathbf{I}}_i) \qquad (1)$$

where $\hat{\mathbf{g}}_i$ is the g-tensor, $\hat{a}_i$ the hyperfine splitting tensor, and $\hat{\mathbf{s}}_i$ and $\hat{\mathbf{I}}_i$ are the electron and nuclear spin operators of the i ion of the triad, respectively. The correlations between the individual g-factors and molecular g-factors for trimers were considered.[5−7,9,10,25,26] The correlations between the effective hyperfine constants and the single-ion hyperfine constants for trimers were also considered.[30,9,25]

For the spin-frustrated clusters with equilateral triangle geometry, considering that the three Cu metals are almost

(12) (a) Costes, J.-P.; Dahan, F.; Lanrent, J.-P. *Inorg. Chem.* **1986**, *25*, 413. (b) Kwiatkowski, M.; Kwiatkowski, E.; Olechnowicz, A.; Ho, D. M.; Deutsch, E. *Inorg. Chim. Acta* **1988**, *150*, 65.
(13) Padilla, J.; Gatteschi, D.; Chaudhuri, P. *Inorg. Chim. Acta* **1997**, *260*, 217.
(14) Azuma, M.; Odaka, T.; Takano, M.; Vander Griend, D. A.; Poeppelmeier, K. R.; Narumi, Y.; Kindo, K.; Mizuno, Y.; Maekawa, S. *Phys. Rev. B* **2000**, *62*, R3588.
(15) Ferrer, S.; Haasnoot, Y. G.; Reedijk, J.; Müller, E.; Cigni, M. B.; Lanfranchi, M.; Lanfredi, A. M. M.; Ribas, J. *Inorg. Chem.* **2000**, *39*, 1859.
(16) Kodera, M.; Tachi, Y.; Kita, T.; Kobushi, H.; Sumi, Y.; Kano, K.; Shiro, M.; Koikawa, M.; Tokii, T.; Ohba, M.; Okawa, H. *Inorg. Chem.* **2000**, *39*, 226.
(17) Clérac, R.; Cotton, F. A.; Dunbar, K. R.; Hillard, E. A.; Petrukhina, M. A.; Smuckler, B. W. *C. R. Acad. Sci., Ser. IIc: Chim.* **2001**, *4*, 315.
(18) Lopes-Sandoval, H.; Contreras, R.; Escuer, A.; Vicente, R.; Bernes, S.; Nöth, H.; Leigh, G. J.; Barba-Berhens, N. *J. Chem. Soc., Dalton Trans.* **2002**, 2648.
(19) Cage, B.; Cotton, F. A.; Dalal, N. S.; Hillard, E. A.; Rakvin, B.; Ramsey, C. M. *J. Am. Chem. Soc.* **2003**, *125*, 5270.
(20) (a) Cannon, R. D.; Jayasooriya, U. A.; Sowrey, F. E.; Tilford, C.; Little, A.; Bourker, J. P.; Rogers, R. D.; Vincent, J. B.; Kearley, G. J. *Inorg. Chem.* **1998**, *37*, 5675. (b) Cannon, R. D.; White, R. P. *Prog. Inorg. Chem.* **1988**, *36*, 195. (c) Cannon, R. D.; Jayasooriya, U. A.; Wu, R.; arapKoske, S. K.; Stride, J. A.; Nielsen, O. F.; White, R. P.; Kearley, G. J.; Summerfield, D. *J. Am. Chem. Soc.* **1994**, *116*, 11869.
(21) Kahn, O. *Chem. Phys. Rev.* **1997**, *265*, 165.
(22) (a) McCusker, J. K.; Schmitt, E. A.; Hendrickson, D. N. In *Magnetic Molecular Materials*; Gatteschi, D., Kahn, O., Miller, J. S., Palacio, F., Eds.; Kluwer: Dordrecht, 1991; p 297. (b) Hendrickson, D. N.; Christou, G.; Schmitt, E. A.; Libby, E.; Bashkin, J. S.; Wang, S.; Tsai, H.-L.; Vincent, J. B.; Boyd, P. D. W.; Huffman, J. C.; Folting, K.; Li, Q.; Streib, W. E. *J. Am. Chem. Soc.* **1992**, *114*, 2455. (c) McCusker, J. K.; Jang, H. G.; Wang, S.; Christou, G.; Hendrickson, D. N. *J. Am. Chem. Soc.* **1991**, *113*, 3012.
(23) Blake, A. B.; Anson, C. E.; arapKoske, S. K.; Cannon, R. D.; Jayasooriya, U. A.; Saad, A. K.; White, R. P.; Summerfield, D. *J. Chem. Soc., Dalton Trans.* **1997**, 2039.
(24) Murao, T. *Phys. Lett.* **1974**, 33.
(25) Cole, J. L.; Clark, P. A.; Solomon, E. I. *J. Am. Chem. Soc.* **1990**, *112*, 9534.
(26) Bencini, A.; Gatteschi, D. *EPR of Exchanged-Coupled Systems*; Springer: Berlin, 1990.
(27) Solomon, E. I.; Baldwin, M. J.; Lowery, M. D. *Chem. Rev.* **1992**, *92*, 521.
(28) Nguyen, H.-H.; Shiemke, A. K.; Jacobs, S. J.; Hales, B. J.; Lingstrom, M. E.; Chan, S. I. *J. Biol. Chem.* **1994**, *269*, 14995.
(29) Spiccia, L.; Graham, B.; Hearn, M. T. W.; Lasarev, G.; Moubaraki, B.; Murray, K. S.; Tiekink, E. R. T. *J. Chem. Soc., Dalton Trans.* **1997**, 4089.
(30) Takano, M. *J. Phys. Soc. Jpn.* **1972**, *33*, 1312.

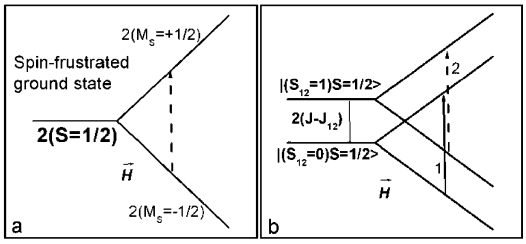

Figure 1. (a) The Zeeman splitting of the degenerate spin-frustrated $2(S = 1/2)$ ground state of the trinuclear Cu_3 cluster with the geometry of an equilateral triangle $J_{12} = J_{13} = J_{23} = J$. (b) The Zeeman splittings and EPR transitions for the $|(0)1/2\rangle$ and $|(1)1/2\rangle$ spin levels of the Cu_3 cluster with the geometry of an isosceles triangle, $J_{12} \neq J_{13} = J_{23} = J$.

structurally equivalent and $J_{12} = J_{13} = J_{23} = J$, the spin Hamiltonian has the form ($H = H_z$)

$$H_0 = -2J(\hat{\mathbf{s}}_1\hat{\mathbf{s}}_2 + \hat{\mathbf{s}}_2\hat{\mathbf{s}}_3 + \hat{\mathbf{s}}_1\hat{\mathbf{s}}_3) + \beta g\hat{s}_Z H_Z + a(\hat{s}_{1Z}\hat{I}_{1Z} + \hat{s}_{2Z}\hat{I}_{2Z} + \hat{s}_{3Z}\hat{I}_{3Z}) \quad (2)$$

We assume that all individual g-factors in the trigonal cluster are equal ($g_1 = g_2 = g_3 = g$) and form the cluster g-factor $g_{||} = g$. The orientations of the single ion hyperfine tensors in the coordinate system of the cluster g-tensor are unknown. Since the hyperfine splittings of the EPR spectra were observed for the parallel cluster g-factor[19,16] and the cluster hyperfine constant ($A_{ZZ} = 157$G[19]) is close to the hyperfine constant of the mononuclear Cu(II) center ($a_{||} = 16-18 \times 10^{-3}$ cm^{-1}), we shall suppose that the local z components of the individual hyperfine tensors are parallel to the molecular Z-axis of the cluster. We assume that all individual hyperfine tensors are equal $a_1 = a_2 = a_3 = a_{zz} = a$ due to the equivalence of the three ions and nuclei in the Cu_3 cluster. Since $a_{zz} \gg a_{xx}, a_{yy}$ for mononuclear Cu(II) centers ($a_{||} = 0.0176$ cm^{-1}, $a_{\perp} \sim 0.0024$ cm^{-1}),[31] we shall consider only Z components of the hyperfine interaction in eq 2.

Many examples have been reported for the Cu_3 clusters with the geometry of an equilateral triangle and strong antiferromagnetic exchange: $J_{ij} = J = -1000 - -20$ cm^{-1}.[4,5,7−9,11−19] In these clusters, strong antiferromagnetic Heisenberg exchange (eq 2) ($J \gg g\beta H \gg a$) results in the degenerate $2(S = 1/2)$ ground state,[4−9,11−18] Figure 1a. The excited $S = 3/2$ level is separated by the interval $3J$ from the ground spin-frustrated state $2(S = 1/2)$. The effective spin Hamiltonian for the $S = 3/2$ level of the trigonal cluster includes the axial operator of zero-field splitting:[31]

$$H' = D_0[\hat{S}_Z^2 - S(S+1)/3] + \beta\hat{\mathbf{S}}\tilde{\mathbf{g}}\mathrm{H}$$

For the Cu_3 cluster with isosceles triangle symmetry $J_{13} = J_{23} = J$, $J_{12} \neq J$, the Heisenberg exchange interaction H_1

$$H_1 = -2J_{12}\hat{\mathbf{s}}_1\hat{\mathbf{s}}_2 - 2J(\hat{\mathbf{s}}_1\hat{\mathbf{s}}_3 + \hat{\mathbf{s}}_2\hat{\mathbf{s}}_3) \quad (3)$$

$$E_1[(S_{12})S] = -J[S(S+1) - 3/4] + (J - J_{12})S_{12}(S_{12}+1)$$

results in the splitting of the four-degenerate spin-frustrated ground state $2(S = 1/2)$ on the separated Kramers doublets $E_1[(S_{12} = 0)S = 1/2] = 0$, $E_1[(S_{12} = 1)S = 1/2] = 2\delta$, $\delta = J - J_{12}$,[5−7,9,10,25,26] which are characterized by the intermediate spin S_{12} ($\mathbf{S}_{12} = \mathbf{s}_1 + \mathbf{s}_2$, $\mathbf{S} = \mathbf{S}_{12} + \mathbf{s}_3$), Figure 1b.

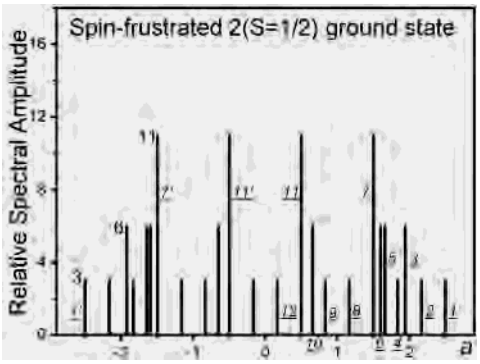

Figure 2. Calculated hyperfine structure of the EPR signal of the spin-frustrated $2(S = 1/2)$ ground state of the Cu_3 cluster with the geometry of an equilateral triangle

In the case of the spin-frustrated trigonal Cu_3 cluster ($J_{ij} = J$, $\delta = 0$), both the $|(S_{12} = 0)S = 1/2\rangle$ and $|(S_{12} = 1)S = 1/2\rangle$ levels have the same energy and form the 4-fold degenerate spin-frustrated ground state $2(S = 1/2)$. In the case $g_i = g$, the Zeeman splittings of the $|(0)1/2\rangle$ and $|(1)1/2\rangle$ levels are the same; the Zeeman $2M_S$ levels of the ground spin-frustrated state $2(S = 1/2)$ are 2-fold degenerate (Figure 1a). Both EPR transitions between these Kramers doublets are characterized by the same molecular g-factor.

The wave functions of the spin-frustrated ground state of the Cu_3 center have the form

$$\chi(S_{12}, S, M_S, m_1, m_2, m_3, M_I) = \Phi[(S_{12})SM_S]\varphi_1(I_1, m_1)\varphi_2(I_2, m_2)\varphi_3(I_3, m_3)$$

where the electronic ground state wave functions $\Phi[(S_{12})SM_S]$ ($S_{12} = 0, 1$; $S = 1/2$, $M_S = \pm 1/2$) diagonalize the Heisenberg exchange Hamiltonian (eqs 2 and 3) and Zeeman interaction. $\varphi_i(I_i,m_i)$ is the nuclear wave function of the i ion, $I_i = 3/2$ for Cu nuclei, the projection $M_I = m_1 + m_2 + m_3$ of the total nuclear spin I has the value $M_I = 9/2(1)$, $7/2(3)$, $5/2(6)$, $3/2(10)$, $1/2(12)$; $\mathbf{I} = \mathbf{I}_1 + \mathbf{I}_2 + \mathbf{I}_3$. To find the hyperfine splittings for the degenerate $2M_S$ Zeeman levels (Figure 1a) of the spin-frustrated ground state $2(S = 1/2)$, it is necessary to diagonalize the hyperfine matrix [128×128] ($2(2I + 1)^3 = 128$). The hyperfine splitting of the spin-frustrated $2M_S$ Zeeman doublets is formed by the hyperfine splittings in the $|(0)1/2\rangle$ and $|(1)1/2\rangle$ doublets and by the hyperfine mixture of the M_I states which belong to these degenerate spin states, since $\langle(0)1/2M_S|\hat{s}_{1Z}\{\hat{s}_{2Z}\}|(1)1/2M_S\rangle = +\{-\}M_S/\sqrt{3}$.

Figure 2 shows the calculated hyperfine structure of the EPR transition (Figure 1a) of the spin-frustrated ground state $2(S = 1/2)$ of the Cu_3 cluster with the geometry of an equilateral triangle. This hyperfine (HF) spectrum consists of the 4 hyperfine lines with intensity 11, 8 HF lines with intensity 6, and 12 HF lines with intensity 3. The relative spectral amplitudes of the 24 hyperfine lines of the total intensity 128 follow the ratio of 3:3:6:3:6:6:11:3:3:6:11:3:

(31) Abragam, A.; Bleavey, B. *Electron Paramagnetic Resonance of Transition Ions*; Clarendon Press: Oxford, 1970.

3:11:6:3:3:11:6:6:3:6:3:3. The extent of this hyperfine spectrum is 5*a*. The positions of the hyperfine lines in Figure 2, their intensities, and corresponding hyperfine components are represented in the Appendix, section a.

In the hyperfine spectrum in Figure 2, the four hyperfine lines 7, 11, 11′, and 7′ (positions $+3a/2$, $+a/2$, $-a/2$, $-3a/2$, respectively) with intensity 11 are separated by the hyperfine intervals *a*. Maximal hyperfine splitting ($\pm 5a/2$) takes place for HF components $\pm 3/2(3)$ (HF line 1) and $\mp 3/2(3)$ (line 1′). The interval between hyperfine lines 2 and 2′ (3 and 3′) is 4.33*a* (3.86*a*). In Figure 2, the hyperfine intervals between the low-intensity HF lines are *a*/3, for example, $\Delta(1,2) = a/3$. The quasidegenerate hyperfine lines 5 and 6 ($\Delta(5,6) = 0.05a$) with intensity 6 are located close to HF line 7 (intensity 11), $\Delta(6,7) = 0.1a$. In the EPR spectrum, these close hyperfine lines (5, 6, and 7) can be observed as one intensive hyperfine line. The positions of the hyperfine lines 3 and 4 {10 and 11} are also close: $\Delta(3,4) = 0.1a$ {$\Delta(10,11) = 0.15a$}, and they can be observed as one hyperfine line. In summary, the resulting calculated hyperfine spectrum of EPR signal of the spin-frustrated ground state $2(S = 1/2)$ represents the complicated hyperfine structure, of extent 5*a*, with hyperfine lines of different intensities, separated by different hyperfine intervals.

Let us consider, for comparison, the hyperfine structures of the EPR transitions 1 and 2 (Figure 1b) of the Kramers doublets $|(S_{12} = 0)S = 1/2\rangle$ and $|(S_{12} = 1)S = 1/2\rangle$, respectively, separated by the exchange interval $2(J - J_{12}) = 2\delta$ in an isosceles Cu_3 triangle (eq 3). The EPR transitions between the $|(0)1/2\rangle$ and $|(1)1/2\rangle$ levels are forbidden. For the $|(0)1/2\rangle$ state, the matrix elements of the spin operators have the form $\langle(0)1/2M_S|\hat{s}_{1Z}[\hat{s}_{2Z}]|(0)1/2M_S\rangle = 0$ and $\langle(0)1/2M_S|\hat{s}_{3Z}|(0)1/2M_S\rangle = M_S$[9,10,25] and only one ion (nonequivalent ion at the vertex of an isosceles triangle) determines the hyperfine splittings. The effective Hamiltonian of the hyperfine interaction for the M_S Zeeman levels of the $|(0)1/2\rangle$ state has the form $H'_{HF} = a\hat{S}_Z\hat{I}_{3Z}$. For EPR transition 1 (Figure 1b), the hyperfine interaction results in four hyperfine peaks with equal spacing, which are represented in Figure 3a.

The relative spectral amplitudes of the four HF lines follow the ratio 16:16:16:16, with total intensity $(2I + 1)^3 = 64$. The positions of the calculated hyperfine peaks are $-3a/2$, $-a/2$, $+a/2$, and $+3a/2$. The intervals between the hyperfine lines are equal to the mononuclear hyperfine constant $A = a$. The length of the hyperfine spectrum is 3*a*. The positions of the hyperfine lines in Figure 3a, their intensities, and corresponding hyperfine components are represented in the Appendix, section b.

For the $|(S_{12} = 1)S = 1/2\rangle$ spin state of an isosceles triangle Cu_3 cluster, the effective Hamiltonian of the hyperfine interaction for the M_S Zeeman levels has the form $H_{HF} = 2a\hat{S}_Z\hat{I}_Z/3 - a\hat{S}_Z\hat{I}_{3Z}$, since $\langle(1)1/2M_S|\hat{s}_{1Z}[\hat{s}_{2Z}]\ |(1)1/2M_S\rangle = 2M_S/3$, $\langle(1)1/2M_S|\hat{s}_{3Z}|(1)1/2M_S\rangle = -M_S/3$ ($\hat{I}_Z$ is the operator of projection of the total nuclear spin). The hyperfine structure of EPR transition 2 (Figure 1b) for the $|(1)1/2\rangle$ level is represented in Figure 3b (—) in comparison with the hyperfine spectrum of EPR transition 1 (—·—).

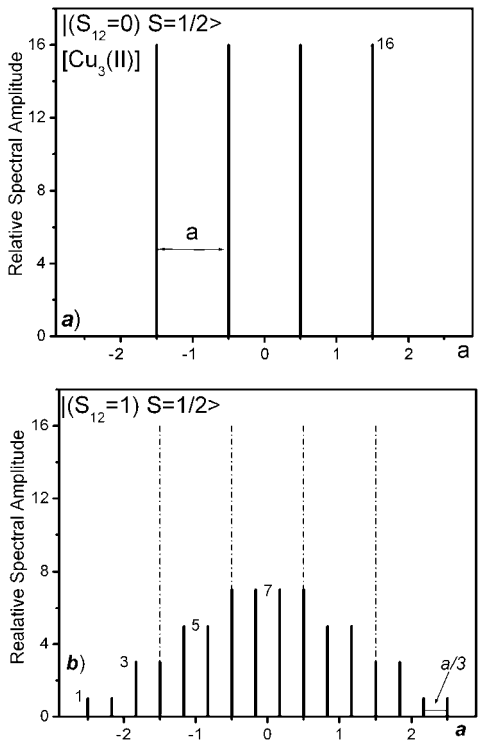

Figure 3. Calculated hyperfine structure of the EPR transitions of two $S = 1/2$ levels of the Cu_3 cluster with the geometry of an isosceles triangle: (a) the $|(S_{12} = 0)S = 1/2\rangle$ level; (b) the $|(S_{12} = 1)S = 1/2\rangle$ level.

The hyperfine spectrum of EPR transition 2 represents the 16 equally spaced hyperfine lines with the spectral intensity distribution 1:1:3:3:5:5:7:7:7:7:5:5:3:3:1:1. The interval between the hyperfine peaks is $A' = a/3$. The total extent of this hyperfine spectrum is 5*a*. Maximal hyperfine splitting $+5a/2$ {$-5a/2$} takes place for hyperfine components $\pm 3/2$ {$\mp 3/2$}. The positions of the hyperfine peaks in Figure 3b, their intensities, and corresponding hyperfine components are represented in the Appendix, section c.

The hyperfine structure (Figure 2) of the EPR transition of the spin-frustrated $2(S = 1/2)$ ground state is not the simple superposition of the hyperfine spectra in Figure 3a,b of EPR transitions 1 ($|(0)1/2\rangle$) and 2 ($|(1)1/2\rangle$) in Figure 1b due to the hyperfine mixture of the degenerate $2M_S$ Zeeman levels of the spin-frustrated $2(S = 1/2)$ state.

In the spin-frustrated cluster ($J_{12} = J_{13} = J_{23} = J$) with different individual g-factors $g_1 = g_2 \neq g_3$, the degeneracy of the $2M_S$ Zeeman levels (Figure 1a) is lifted: $E_{II}[(1)1/2M_S] - E_I[(0)1/2M_S] = 2(g_1 - g_3)\beta HM_S/3$. There are two allowed EPR transitions I and II with g-factors $g_I(S_{12} = 0) = g_3$ and $g_{II}(S_{12} = 1) = (2g_1 + g_3)/3$. In the case when $|g_1 - g_3|\beta H/3 \gg a$, the hyperfine splittings of EPR signals I and II have the form represented in Figure 3a,b, respectively.

Figure 4 shows the hyperfine structure of the allowed EPR transitions $|S = 3/2, M_S = -3/2\rangle \rightarrow |3/2, -1/2\rangle$, $|S = 3/2, -1/2\rangle \rightarrow |S = 3/2, 1/2\rangle$ and $|S = 3/2, 1/2\rangle \rightarrow |S = 3/2, 3/2\rangle$ for the $S = 3/2$ state of the Cu_3 cluster. For the $S = 3/2$ state, the correlation $\langle|s_{iZ}|\rangle = M_S/3$, $i = 1, 2, 3$, takes place for each vertex of the Cu_3 triangle and the effective Hamiltonian of the hyperfine interaction has the form $H^*_{HF} = a\hat{S}_Z\hat{I}_Z/3$ for this $S = 3/2$ level.

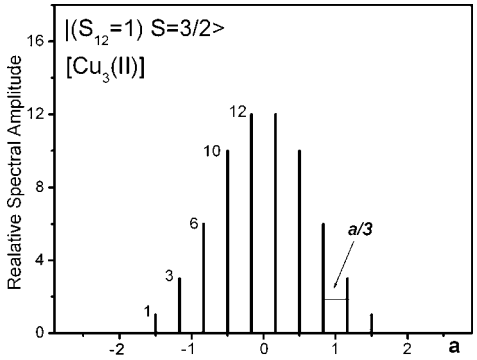

Figure 4. The hyperfine structure of EPR signals of the excited $S = 3/2$ state of the Cu_3 cluster.

The hyperfine spectrum (Figure 4) represents the 10 equally spaced hyperfine peaks with the follow spectral intensity distribution: 1[HF component ∓9/2]:3[∓7/2]:6[∓5/2]:10[∓3/2]:12[∓1/2]:12[±1/2]:10[±3/2]:6[±5/2]:3[±7/2]:1[±9/2]. The interval between the hyperfine lines is $A^* = a/3$. The total length of the hyperfine spectra is $3a$. Maximal hyperfine splitting $+3a/2$ [$-3a/2$] takes place for hyperfine components ±9/2 [∓9/2]. In comparison with the hyperfine spectra in Figures 2 and 3, all the same HF components belong to the single hyperfine line in Figure 4. The hyperfine structure for the EPR transitions in the $S = 3/2$ exchange level does not depend on the symmetry of the Cu triangle and corresponds to the ferromagnetic ordering of all spins in the trimer.

The authors[19] supposed that the ground state of the spin-frustrated trigonal Cu triangle is the doublet $S = 1/2$ and the EPR transition is characterized by the hyperfine spectrum which consists of 10 hyperfine peaks. However, the HF spectrum of the EPR transition in the spin-frustrated $2(S = 1/2)$ ground state of the trigonal Cu triangle has the form represented in Figure 2 due to the degeneracy of the $2(S = 1/2)$ ground state.

In the case of the scalene cluster ($J_{12} \neq J_{13}$, $J_{12} \neq J_{23}$, $J_{13} \neq J_{23}$), the splitting between two Kramers doublets is $\Delta_1 = E_1(1/2) - E_2(1/2) = 2[J_{12}^2 + J_{13}^2 + J_{23}^2 - J_{12}J_{13} - J_{12}J_{23} - J_{13}J_{23}]^{1/2}$.[5,30,9,10,25] Each Kramers doublet is the mixture of the $|(0)1/2\rangle$ and $|(1)1/2\rangle$ states which depends on the exchange parameter[9,10,25] $\alpha = (2J_{12} - J_{13} - J_{23})/\Delta_1$: $\Psi_{1,2}(1/2) = c_{\pm}|(1)1/2\rangle \mp c_{\mp}|(0)1/2\rangle$, $c_{\pm} = \sqrt{(1 \pm \alpha)/2}$. For the scalene Cu_3 cluster with $g_1 = g_2 = g_3 = g$, the EPR transitions between the Kramers doublets are forbidden. The effective hyperfine constants[25] and hyperfine splittings strongly depend on relations J_{13}/J_{12} and J_{23}/J_{12}. The hyperfine spectrum of the EPR signal for the ground state of the scalene Cu_3 site $\Psi_2(1/2) = 0.269|(1)1/2\rangle + 0.966|(0)1/2\rangle$ ($J_{13}/J_{12} = 0.9$, $J_{23}/J_{12} = 0.8$) is represented in Figure 5 in comparison with the hyperfine structure of the EPR signal of the pure $|(0)1/2\rangle$ level ($-\cdot-$). The slight scalene deformation ($J_{13}/J_{23} = 1.125$) of an isosceles Cu_3 cluster results in the disappearance of the high-intensity quartet hyperfine spectrum characteristic of the $|(0)1/2\rangle$ level (Figure 5).

In the trigonal spin-frustrated Cu_3 cluster ($J_{12} = J_{13} = J_{23} = J$) with degenerate $2(S = 1/2)$ ground state, the Dzialoshinsky−Moriya antisymmetric exchange interactions[32] (eq 4)

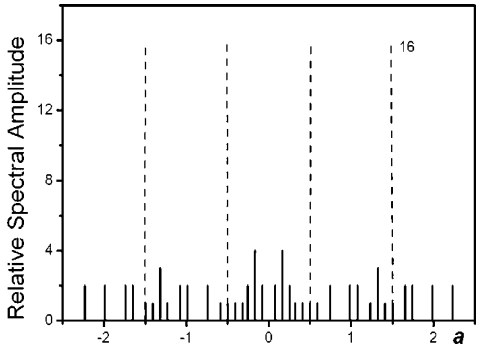

Figure 5. The hyperfine structure of the EPR signal of the ground $S = 1/2$ state of the scalene Cu_3 cluster: $J_{13}/J_{12} = 0.9$, $J_{23}/J_{12} = 0.8$.

$$H_{DM} = D_{12}^Z[\vec{s}_1 \times \vec{s}_2]_Z + D_{23}^Z[\vec{s}_2 \times \vec{s}_3]_Z + D_{31}^Z[\vec{s}_3 \times \vec{s}_1]_Z \quad (4)$$

splits the degenerate $2(S = 1/2)$ state.[7,9] (The Dzialoshinsky−Moriya antisymmetric exchange determines the chiral vector $\vec{k} = 2([\vec{s}_1 \times \vec{s}_2] + [\vec{s}_2 \times \vec{s}_3] + [\vec{s}_3 \times \vec{s}_1])/3\sqrt{3}$ in the geometrically frustrated magnetic systems: kagomé lattices that are composed of equilateral triangles of transition metals.[33]) The splitting of the degenerate $2(S = 1/2)$ ground state by the Dzialoshinsky−Moriya antisymmetric exchange has the form $E_{\pm}(1/2) = \pm\sqrt{3}G_Z/2$, where the cluster vector parameter $G_Z = (D_{12}^Z + D_{23}^Z + D_{31}^Z)/3$ is directed along the trigonal Z-axis of the trigonal Cu_3 cluster.[7,9] The wave functions which diagonalize the Dzialoshinsky−Moriya antisymmetric exchange (eq 4) for the trigonal Cu_3 cluster have the form $\Phi_{\pm}(1/2) = [|(0)1/2\rangle \pm i|(1)1/2\rangle]/\sqrt{2}$. In the case of the splitting of the spin-frustrated $2(S = 1/2)$ state by the antisymmetric exchange (eq 4), EPR transitions are allowed in the $E_+(1/2)$ and $E_-(1/2)$ doublets and also between the $E_-(1/2)$ and $E_+(1/2)$ levels. All three ions are equivalent in the $E_+(1/2, M_S)$ and $E_-(1/2, M_S)$ states: $\langle\Phi_{\pm}(1/2,M_S)|\hat{s}_{1Z}|\Phi_{\pm}(1/2,M_S)\rangle = \langle|\hat{s}_{2Z}|\rangle = \langle|\hat{s}_{3Z}|\rangle = M_S/3$. In this case, the effective Hamiltonian of the hyperfine interaction has the form $H_{HF}^* = a\hat{S}_Z\hat{I}_Z/3$ for the $E_{\pm}(1/2)$ Kramers levels. The hyperfine structure of all EPR signals ($H = H_Z$) of the $E_{\pm}(1/2)$ levels has the form of the 10 hyperfine lines with equal spacing ($A^* = a/3$) which follow the spectral intensity distribution 1:3:6:10:12:12:10:6:3:1 and with total length $3a$, represented in Figure 4.

Discussion

The hyperfine spectra (Figures 2−5) of the EPR transitions of the spin-frustrated trigonal Cu_3 cluster, isosceles triangle, and totally distorted (scalene) Cu trimers are essentially different. The hyperfine spectrum of EPR transition 1 of the $|(S_{12} = 0)S = 1/2\rangle$ level represents the well resolved quartet of equally spaced hyperfine lines of the same high intensity (16) with the interline interval $A = a$. A comparison of this calculated hyperfine spectrum (Figure 3a) and hyperfine

(32) (a) Dzyaloshinsky, I. *Phys. Chem. Solids* **1958**, *4*, 241. (b) Moriya, T. *Phys. Rev.* **1960**, *117*, 635; *120*, 91.
(33) (a) Elhajal, M.; Canals, B.; Lacroix, C. *Phys. Rev. B* **2002**, *66*, 014422. (b) Nishiyama, M.; Maegawa, S.; Inami, T.; Oka, Y. *Phys. Rev. B* **2003**, *67*, 224435.

splitting (Figure 2) of the ground $2(S = 1/2)$ state of the spin-frustrated trigonal cluster with the hyperfine structure[19] of the spin-frustrated Cu_3 cluster, which is characteristic of a single Cu(II) nucleus, indicates that the hyperfine structure observed in the EPR experiment[19] can be attributed to the $|(S_{12} = 0)S = 1/2\rangle$ level of the isosceles triangle. Since $\langle|s_{1Z}[s_{2Z}]||\rangle = 0$ and $\langle|s_{3Z}|\rangle = M_S$ for the $|(0)1/2\rangle$ level, only one Cu ion (s_3) forms the molecular g-factor and hyperfine structure in this state.[9,10,25] As noted,[25] for the $|(0)1/2\rangle$ level of the isosceles Cu trimer, the paramagnetism will be localized on the one Cu ion and the EPR of the trimer will only reflect the properties of this ion.

The single EPR transition $2'$ in the ground state doublet $S = 1/2$ was discussed in ref 19 since the doublet $S = 1/2$ was considered[19] as the spin-frustrated ground state of the Cu_3 cluster with the geometry of an equilateral triangle. However, the degenerate $2(S = 1/2)$ two-doublets state is the spin-frustrated ground state of the Cu_3 cluster with the geometry of an equilateral triangle. If the observed[19] HF structure belongs to the $|(0)1/2\rangle$ level (EPR transition 1 in Figure 1b), the EPR transition 2 (Figure 1b) of the $|(1)1/2\rangle$ level should be observed also. The EPR transition of the second $S = 1/2$ doublet of the spin-frustrated $2(S = 1/2)$ ground state was not considered in ref 19. For explanation of the single $S = 1/2$ EPR signal,[19] one can suppose that the exchange splitting $2\delta = 2(J - J_{12})$ between the $|(0)1/2\rangle$ and $|(1)1/2\rangle$ levels may be very small (for example, $2|\delta| = 0.1-1$ cm^{-1}) and EPR transitions 1 and 2 (Figure 1b) can be observed as the single EPR signal. At the same time, this exchange splitting 2δ, being essentially stronger than the hyperfine splittings ($\delta \gg a$), is enough to destroy the hyperfine structure (Figure 2) of the spin-frustrated $2(S = 1/2)$ ground state EPR and form two separate EPR transitions with the hyperfine spectra characteristic of the $|(S_{12} = 0)S = 1/2\rangle$ (Figure 3a) and $|(S_{12} = 1)S = 1/2\rangle$ (Figure 3b) states. In the case of relatively small δ splittings, both transitions, 1 and 2, take place in the EPR spectra with their hyperfine structures. The well resolved quartet hyperfine structure, with total length $3a$, of the $|(S_{12} = 0)S = 1/2\rangle$ level may be observed due to the large interval $A = a$ between hyperfine peaks. In the EPR spectra[19] of the doublet state of the Cu_3 spin-frustrated cluster, the well resolved quartet hyperfine structure was observed with $A = 157$ G which exceeds the ΔH_{pp} peak-to-peak line width $= 116$ G.[19] At the same time, the hyperfine structure (Figure 3b) with total length $5a$ of EPR transition 2 of the $|(S_{12} = 1)S = 1/2\rangle$ level may be not resolved in these conditions since the hyperfine intervals between the hyperfine lines is $A' = a/3$ ($\sim$50 G) in this case. One can note that nonobservation of the hyperfine structure of the type in Figure 4 for EPR transitions in the excited Cu_3 $S = 3/2$ state (EPR transitions 1, 2 and 3[19]) is the argument in favor of this assumption. Indeed, as follows from Figure 4, the hyperfine structure for all EPR transitions in the $S = 3/2$ level represents the 10 hyperfine lines with the HF interline interval $A^* = a/3$, the same as $A' = a/3$ in the HF spectrum in Figure 3b for the $|(1)1/2\rangle$ level. Hyperfine structures with this HF interval ($a/3$) were not observed for the EPR transitions in the $S = 3/2$ level.[19]

In summary, the observed[19] quartet hyperfine structure is not described by the spin-frustrated hyperfine structure (Figure 2). In the spin-coupling model, the observed[19] hyperfine structure corresponds to EPR transition 1 of the $|(0)1/2\rangle$ level (Figure 3a) of an isosceles Cu trimer; the hyperfine structure of the second EPR transition of the $|(1)1/2\rangle$ level (Figure 3b) was not resolved.

The correlation between the high magnetic symmetry ($J_{ij} = J$), which corresponds to the crystallographic symmetry of the cluster, and the possibility of small distortions ($\delta \neq 0$) of the trigonal metal centers is an important point for the spin-frustrated clusters. In all spin-frustrated trigonal or quasi-trigonal Cu_3 clusters,[4−19] the variable-temperature magnetic susceptibility $\chi(T)(\mu_{eff}(T))$ was described by a single Heisenberg exchange parameter $J_{12} = J_{13} = J_{23} = J$. However, the small splittings 2δ of the spin-frustrated $2(S = 1/2)$ ground state on the two separated Kramers doublets $|(S_{12} = 0)S = 1/2\rangle$ and $|(S_{12} = 1)S = 1/2\rangle$ (or two doublets of the scalene triangle) may not be determined by the susceptibility measurements even at low temperatures. The susceptibility may be described by some sets of exchange parameters.[10,14,25,29] Thus, for example, the magnetic susceptibility of the Cu_3 clusters in $La_4Cu_3MoO_{12}$ was described by $J_{12} = J_{13} = J_{32} = -282.5$ cm^{-1}.[14] At the same time, the authors[14] note that calculated magnetic susceptibility did not change significantly even when $2|\delta| = 2|J_{12} - J| \approx 35$ cm^{-1} like $J_{12} = -294$ cm^{-1}, J $(=J_{13} = J_{23}) = -276.5$ cm^{-1} for an isosceles triangle and $J_{13}/J_{12} = 1.13$, $J_{23}/J_{12} = 1.07$, $J_{12} = -266$ cm^{-1} for the scalene triangle ($\Delta_1 = 60.5$ cm^{-1}); i.e., there is some uncertainty (flexibility) of the exchange parameters determined from $\chi(T)$ in the spin-frustrated cluster.

An analogous problem of correlation between the trigonal cluster symmetry and distortions in spin-frustrated Cr_3(III) and Fe_3(III) basic carboxylate clusters was discussed.[9,20] In these clusters, the magnetic susceptibility was described by a single exchange parameter J. However, the low-temperature spin-heat capacity,[34] inelastic neutron scattering,[35,20] and Mössbauer spectra[30] of the spin-frustrated trimeric basic carboxylates demonstrate small deviations $\delta = 1-5$ cm^{-1} of the magnetic parameters from the trigonal scheme $J_{12} = J_{13} = J_{23} = J$.

For the Cu_3 clusters[14] with $J = -282.5$ cm^{-1} in $La_4Cu_3MoO_{12}$, the spin-heat capacity measurements[14] show that the degeneracy of the two Kramers doublets with $S = 1/2$ is lifted by a slight distortion of the trigonal cluster.

As follows from the results of the spin-coupling model of hyperfine interactions for the spin-frustrated (Figure 2) and distorted (Figure 3) Cu_3 clusters, the observation[19] of the well resolved quartet hyperfine structure of the EPR signal of the Cu_3 spin-frustrated cluster may be considered as evidence of symmetry lowering, and the splitting of the $2(S = 1/2)$ ground manifold on the $|(S_{12} = 0)S = 1/2\rangle$ and $|(S_{12} = 1)S = 1/2\rangle$ Kramers doublets. In the case of the

(34) Sorai, M.; Tachiki, M.; Suga, H.; Seki, S. *J. Phys. Soc. Jpn.* **1971**, *30*, 75.
(35) (a) Furrer, A.; Güdel, H. U. *Helv. Phys. Acta* **1977**, *50*, 439. (b) Furrer, A.; Güdel, H. U. *Phys. Rev. Lett.* **1977**, *39*, 657.

small splitting $2\delta \sim g\beta H$, it is difficult to determine the $|(S_{12})S = 1/2\rangle$ ground state and interval 2δ from the EPR spectra. Spin-heat capacity and inelastic neutron scattering experiments can provide information about the splitting and symmetry of this spin-frustrated Cu_3 complex. In the case of strong δ-splitting $2\delta \gg g\beta H$, the two EPR signals 1 and 2 with different hyperfine structure and length ($3a$ and $5a$), and different temperature dependence may be observed.

Observation of the quartet hyperfine structure in the Cu_3 complex[19] shows also that the symmetry of the Cu_3 cluster in this case is the isosceles triangle with $J_{12} \neq J = J_{13} = J_{23}$ and not the scalene cluster when the high symmetrical quartet hyperfine structure is destroyed by a slight scalene type distortion of the isosceles Cu_3 cluster (Figure 5). The observed quartet hyperfine structure also demonstrates that the Dzialoshinsky−Moriya antisymmetric exchange (with the hyperfine spectrum in Figure 4 for the $S = 1/2$ doublets) is absent in this cluster due to the symmetry conditions ($G_Z = 0$) or is strongly reduced by the isotropic distortion ($\delta \gg G_Z$).

The variable-temperature magnetic susceptibility of the three $[Cu_3(M_3{-}OH)L_3A(H_2O)_2]A{\cdot}(H_2O)_x$ complexes[15] was described in the spin-frustrated model ($J_{12} = J_{13} = J_{23} = J$) with strong antiferromagnetic exchange $J \sim 190{-}198$ cm^{-1}. The observed fine structure of the axial solid state EPR spectra of the spin-frustrated ground state was described[15] by the hyperfine coupling constant $A_{||} = 135{-}151 \times 10^{-4}$ cm^{-1}, which is close to $A_{||}$ characteristic of a single Cu nucleus. This hyperfine characteristic of the spin-frustrated $2(S = 1/2)$ ground state may also be explained in the spin-coupling model with small δ distortion and the EPR spectra of the $|(S_{12} = 0)S = 1/2\rangle$ level with quartet hyperfine structure, Figure 3a.

The parallel component of the EPR signal of the ground $2(S = 1/2)$ state of the $[Cu_3(Br)(L1O)_3](PF_6)_2$ spin-frustrated complex[16] with $J = -19.5$ cm^{-1} is characterized by the hyperfine structure of the four hyperfine lines.[16] The authors did not explain the hyperfine structure. They note that the hyperfine splitting is a complicated multiplet and is broadened due to a spin delocalization between the three Cu atoms. The observed[16] well resolved hyperfine structure can also be described as the hyperfine structure characteristic of the $|(S_{12} = 0)S = 1/2\rangle$ level. The EPR spectra of the other spin-frustrated $[Cu_3(X)(LnO)_3](PF_6)_2$ complexes[16] with small J values ($J = -0.3 - -4.8$ cm^{-1}) demonstrate more complicated well resolved hyperfine structures and require consideration of the superposition of the hyperfine spectra of the two $S = 1/2$ levels and S = 3/2 level.

The calculated hyperfine structures (Figure 3a,b) may be used for consideration of the hyperfine structure of the EPR transitions of the $S = 1/2$ levels of an isosceles Cu_3 triangle. The magnetic susceptibility of the Cu_3 complex[29] with various Cu···Cu distances (3.56, 4.56, 5.47 Å) was described in the model of the isosceles triangle with $J_{12} = -53$ cm^{-1} (or ca. -80 cm^{-1}) and $J = -90$ cm^{-1} (or -77 to -90 cm^{-1}), $E[(0)1/2] - E[(1)1/2] = 74$ cm^{-1}.[29] For an explanation of the six equally spaced hyperfine components of the EPR powder spectra ($T = 77$ K) with the separation of 77 G, the authors[29] proposed two possibilities: (1) the hyperfine structure of the Cu_2 exchange pair or (2) the superposition of $S = 1/2$ signals from both the ground $|(S_{12} = 1)S = 1/2\rangle$ and excited $|(S_{12} = 0)S = 1/2\rangle$ levels of an isosceles Cu triangle, both of which are thermally accessible at 77 K. Consideration of the two calculated hyperfine spectra in Figure 3a,b, which are characteristic of the essentially separated ground $|(1)1/2\rangle$ and excited $|(0)1/2\rangle$ levels, shows that any superposition of these two hyperfine spectra cannot produce the resulting observed[29] hyperfine spectrum of the six or seven equally spaced HF lines with the interline separation $\sim a/2$. This analysis excludes the second proposed explanation of observed[29] hyperfine spectra of the Cu triangle. For more detailed analysis, it is necessary to measure the hyperfine spectra at low temperature.

Solutions of the trinuclear Cu(II) clusters yield hyperfine spectra characteristic of mononuclear copper(II) complexes.[12a,29] The observation of this mononuclear-type hyperfine structure with the interline interval $A \sim a$ was interpreted[29] as an indication that dissolution results in the formation of uncoupled copper(II) centers. At the same time, the authors[29] confirm the persistence of the trinuclear Cu_3 units in solution. The quartet hyperfine structure, characteristic of a Cu(II) monomer, was observed in the solid state EPR[19] of the ground $S = 1/2$ state of the Cu_3 units. This hyperfine structure is characteristic of the $|(S_{12} = 0)S = 1/2\rangle$ level of the isosceles Cu triangle (Figure 3a). The possibility of observation in solution of the isosceles Cu triangles with the hyperfine spectra of the $|(S_{12} = 0)S = 1/2\rangle$ level, which are the same as for a Cu(II) monomer, should be taken into account in interpretation of the hyperfine structure of the EPR spectra of the Cu_3 clusters in solutions.

For dimeric Cu(II) clusters,[36] the spin-coupling model describes the observed hyperfine structure: the 7 equidistant ($A = a/2$) hyperfine lines with intensities 1:2:3:4:3:2:1 for the EPR transitions in the triplet state. Figures 2−5 show that the spin-coupling model describes also the hyperfine structures of EPR spectra of all spin levels of the Cu_3 clusters with geometries of equilateral, isosceles, and scalene triangles. The spin-coupling model of hyperfine splittings provides the correlations between the hyperfine structures and magnetic symmetry of the trinuclear Cu_3 clusters.

Conclusion

The hyperfine structures of the EPR transitions are very specific for the spin-frustrated Cu_3 clusters with geometries of an equilateral triangle and distorted isosceles and scalene copper trimers. The quartet hyperfine structure, characteristic of a single Cu^{2+} nucleus, which was observed experimentally for the $S = 1/2$ ground state of the spin-frustrated Cu_3(II) clusters, corresponds to the $|(S_{12} = 0)S = 1/2\rangle$ level of an isosceles Cu triangle. This hyperfine structure is evidence of the symmetry lowering from an equilateral to an isosceles Cu triangle and small splitting of the spin-frustrated $2(S = 1/2)$ ground-state manifold.

(36) (a) Bleany, B.; Bowers, K. D. *Proc. R. Soc. London* **1952**, *A214*, 451. (b) Abe, H.; Shimada J. *Phys. Rev.* **1953**, *90*, 316. (c) Kokoszka, G. F.; Duerst, R. W. *Coord. Chem. Rev.* **1970**, *5*, 209.

Appendix: Positions of the Hyperfine Lines, Their Intensities, and Corresponding Hyperfine Components

(a) The Spin-Frustrated 2($S = 1/2$) Ground State of an Equilateral Triangle Cu_3 Cluster (Figure 2). The total spectral amplitudes (in brackets) of the hyperfine lines 1−12 in the right part of Figure 2, positions and corresponding hyperfine components, are the following: 1[3] $+5a/2$, $\pm 3/2(3)$; 2[3] $+13a/6$, $\pm 5/2(3)$; 3[6] $+1.93a$, $\pm 1/2(6)$; 4[3] $+11a/6$, $\pm 7/2(3)$; 5[6] $1.65a$, $\pm 3/2(6)$; 6[6] $+1.60a$, $\mp 1/2(6)$; 7[11] $+3a/2$, $\pm 9/2(2)$, $\pm 5/2(3)$, $\pm 1/2(3)$, $\mp 3/2(3)$; 8[3] $+7a/6$, $\mp 1/2(3)$; 9[3] $5a/6$, $\pm 1/2(3)$; 10[6] $+0.65a$, $\mp 3/2(6)$; 11[11] $+3a/2$, $\pm 7/2(3)$, $\pm 3/2(2)$, $\mp 1/2(3)$, $\mp 5/2(3)$; 12[3] $+a/6$, $\pm 5/2(3)$.The positions of the hyperfine lines 1′−12′ (left part of Figure 2a) and hyperfine components are obtained by the change of the corresponding sign. The degeneracy (n) of the hyperfine components is determined by the nuclear spin sets $\varphi_1(I_1,m_1)\varphi_2(I_2,m_2)\varphi_3(I_3,m_3) = |m_1, m_2, m_3\rangle$ which results in M_I. The specific hyperfine characteristic of the spin-frustrated 2($S = 1/2$) state is the fact that all analogous [different] nuclear spin sets $|m_1, m_2, m_3\rangle$ with the same fixed M_I contribute to the same [different] hyperfine lines. Thus, for example, the hyperfine splittings for the three analogous nuclear spin sets $|3/2, 3/2, -3/2\rangle$, $|3/2, -3/2, 3/2\rangle$, and $|-3/2, 3/2, 3/2\rangle$ (and corresponding $|-m_1, -m_2, -m_3\rangle$ sets) form HF line 1 with intensity 3 (position $+5a/2$, Figure 2) and contribute to HF line 7′ (position $-3a/2$). On the other hand, the hyperfine splittings for the other six analogous nuclear spin sets $|m_i = 3/2, m_j = 1/2, m_k = -1/2\rangle$ with $M_I = 3/2$ result in hyperfine lines 5 (position $1.65a$, Figure 2) and 10′ (position $-0.65a$) with intensity 6. The HF splitting of the third possible nuclear spin set $|1/2, 1/2, 1/2\rangle$ with $M_I = 3/2$ contributes to hyperfine line 11 (position $a/2$, Figure 2).

(b) The Kramers Doublet $|(S_{12} = 0)S = 1/2\rangle$ of an Isosceles Cu_3 Triangle (Figure 3a). The hyperfine components, which correspond to the hyperfine line at position $+3a/2$ $\{+a/2\}$ in Figure 3a, are the following: $\mp 3/2(1)$, $\mp 1/2(2)$, $\pm 1/2(3)$, $\pm 3/2(4)$, $\pm 5/2(3)$, $\pm 7/2(2)$, $\pm 9/2(1)$ $\{\mp 5/2(1)$, $\mp 3/2(2)$, $\mp 1/2(3)$, $\pm 1/2(4)$, $\pm 3/2(3)$, $\pm 5/2(2)$, $\pm 7/2(1)\}$. The hyperfine components, which correspond to the hyperfine line at position $-3a/2$ $\{-a/2\}$, have opposite signs. The same hyperfine components $\pm M_I$ belong to different hyperfine lines.

(c) The Kramers Doublet $|(S_{12} = 1)S = 1/2\rangle$ of an Isosceles Cu_3 Triangle (Figure 3b). The total spectral amplitudes (in parentheses [ ]), positions of the 8 hyperfine lines in the right part of Figure 3b, and corresponding hyperfine components are the following: 1[1] $+5a/2$, $\pm 3/2(1)$; 2[1] $+13a/6$, $\pm 5/2(1)$; 3[3] $+11a/6$, $\pm 7/2(1)$, $\pm 1/2(2)$; 4[3] $+3a/2$, $\pm 9/2(1)$, $\pm 3/2(2)$; 5[5] $+7a/6$, $\pm 5/2(2)$, $\mp 1/2(3)$; 6[5] $+5a/6$, $\pm 7/2(2)$, $\pm 1/2(3)$; 7[7] $+a/2$, $\pm 3/2(3)$, $\mp 3/2(4)$; 8[7] $+a/6$, $\pm 5/2(3)$, $\mp 1/2(4)$. For the 8 hyperfine lines in the left part of Figure 3b, the positions and corresponding hyperfine components have the opposite sign.

IC035141R